JGR Atmospheres

RESEARCH ARTICLE
10.1029/2018JD029817

Lightning Initiation Processes Imaged With Very High Frequency Broadband Interferometry

Fanchao Lyu[1], Steven A. Cummer[1], Zilong Qin[2], and Mingli Chen[2]

[1]Electrical and Computer Engineering Department, Duke University, Durham, NC, USA, [2]Department of Building Service Engineering, Hong Kong Polytechnic University, Hung Hom, Hong Kong

Key Points:
- Lightning initiation processes imaged at close range with a new VHF broadband interferometer can be classified into two different groups
- The first is the reported fast positive breakdown, with 10–20 μs continuous VHF bursts that merge continuously into upward negative leaders
- The second is a kind of isolated short VHF pulses of typical duration <0.5 μs that begin hundreds of microseconds prior to upward negative leader

Correspondence to:
S. A. Cummer,
cummer@ee.duke.edu

Citation:
Lyu, F., Cummer, S. A., Qin, Z., & Chen, M. (2019). Lightning initiation processes imaged with very high frequency broadband interferometry. *Journal of Geophysical Research: Atmospheres*, *124*, 2994–3004. https://doi.org/10.1029/2018JD029817

Received 12 OCT 2018
Accepted 20 FEB 2019
Accepted article online 27 FEB 2019
Published online 18 MAR 2019

Abstract Recent measurements of narrow bipolar lightning events (NBEs) by very high frequency (VHF) radio interferometer have resolved the dynamic development of this special lightning process with submicrosecond time resolution, and showed that the fast positive breakdown (FPB) process is responsible for initiating at least some lightning flashes. In this study, with a newly built and deployed VHF interferometer system, we analyzed 31 intracloud lightning flash initiation events during three thunderstorms at short range from the interferometer. These events separate into two distinct classes that can be identified based on the time scale and the occurrence contexts of the first detectable VHF emissions from the flash. One class has features completely consistent with previously reported FPB events and is associated with continuous VHF emissions of 10–20 μs duration. Downward motion of the FPB region centroid merged continuously into the development of the subsequent upward negative leaders. But the majority of the lightning flashes analyzed began with ultrashort, submicrosecond duration, isolated pulses of VHF emission with no identifiable FPB signatures between these pulses and the leader development. These short VHF pulses begin typically a few hundred microseconds before the upward leader developes and are located at the same position where the leader eventually begins. We suggest that the FPB process is responsible for initiating some but not all lightning flashes, and the extremely short pulse-like VHF emissions play a role in initiating those flashes without any FPB process.

1. Introduction

The initiation of lightning, which is almost always hidden deep inside thunderclouds, has been proven to be challenging to understand because of the difficulty of direct measurements. Since the identification of narrow bipolar events (NBEs) or compact intracloud discharges (CIDs; Smith et al., 1999), they have been a strong research focus because of their intrinsic link to the initiation of some intracloud flashes (ICs; Rison et al., 1999; Smith et al., 1999) and their unusual and strong radio low- and high-frequency radio emissions (Le Vine, 1980; Smith et al., 1999; Willett et al., 1989). Recently, new insights into lightning initiation were revealed by observations of NBEs using very high frequency (VHF) interferometers (Liu et al., 2012; Rison et al., 2016). With an upgraded continuous VHF interferometer (Stock et al., 2014), the dynamic development of a process called fast positive breakdown (FPB) was identified and was observed to be associated with not only typical NBEs but also the initiation of some normal ICs and cloud-to-ground flashes (CGs; Rison et al., 2016). Both a "weak version" and "strong version" of FPB, associated with weak and strong electric field pulses were observed. The FPB process was suggested to be the initiation of many and perhaps most lightning flashes (Rison et al., 2016) and thus supports the positive streamer lightning initiation mechanism (Griffiths & Phelps, 1976; Phelps, 1974).

On the other hand, from electric field sensor observations of the initial electric field change of CG and IC flashes at close range, Marshall et al. (2014) and Chapman et al. (2017) reported a type of initiation event that they named as initial electric field change (IEC). These IEC events were observed at the very beginning of both IC and CG flashes from the electric field change measurements, with a time scale of several hundred microseconds to several milliseconds. However, no typical NBE was detected in their studies except for a few cases of a weak NBE-like pulse (Chapman et al., 2017). Chapman et al. (2017) and Rison et al. (2016) suggested that this was consistent with a "wide range of the strength of the fast positive breakdown." Chapman et al. (2017) further suggested that "IEC is a fundamental part of all or almost all lightning initiations and that IEC is needed prior to the first initial breakdown pulse." The findings by Marshall et al. (2014) and Chapman et al. (2017) were recently expanded by Marshall et al. (2018), which was published while this

study was in review, with measurements of electric field change and narrowband VHF (bandwidth of 186–192 MHz, named as LogRF). Marshall et al. (2018) analyzed two intracloud and two cloud-to-ground lightning flashes and found that the IEC initiation was coincident with a short pulse in the LogRF data.

The pictures of lightning initiation painted by Rison et al. (2016) and Chapman et al. (2017) are not entirely consistent. It is possible that the observed IECs might occur after weak FPBs, when there are no NBE-type bipolar pulses observed (Chapman et al., 2017). However, details of the basic signature of the radio frequency emissions associated with non-NBE lightning initiation is still unclear. Furthermore, it is known that typical NBEs are present in only a small fraction of the total lightning flashes (e.g., the statistics summarized by Lü et al., 2013; and references therein), so perhaps it is not the case that all lightning flashes initiate with a burst of FPB. Accordingly, more investigation of the radio emissions associated with lightning initiation is needed, especially for those flashes that started without typical NBEs and clear FPB, to better understand the basic radio emission signature and the physical mechanism (or mechanisms) of lightning initiation.

Our goal here is to document all of the processes associated with the initiation of lightning flashes (IC flashes in current study), including FPB, and to assess how frequently FPB and flash initiation occur simultaneously. A VHF broadband interferometer system (e.g., Kawasaki et al., 2000, Shao et al., 1996, 2018, , Stock et al., 2014, Sun et al., 2013) was built and deployed at Duke Forest (DF) near Duke University in Durham, North Carolina (NC) in 2017 in order to image lightning leader development on microsecond time scales. A brief introduction into the interferometer system and preliminary results on the understanding of the initiation process of lightning have been presented in earlier conference papers (Cummer et al., 2018a, 2018b). Here we extended the preliminary analysis by thoroughly investigating a total of 31 IC flashes from three different storms that initiated close to our system, which lets us to paint a more complete picture on the initiation of lightning flashes. All of these flashes started with detectable VHF emissions. Two classes of initiation were identified based primarily on the time scale of the VHF emissions. One class is unquestionably the same as the recently reported FPB process (Rison et al., 2016) that produces continuous VHF emissions on time scale of approximately 10–20 μs. Some of these exhibited clear downward motion (Rison et al., 2016) while others were too weak to be spatially resolved. The other class is characterized by isolated, short VHF pulses of typical duration <0.5 μs that occur typically several hundred microseconds before the main upward leader development. These short and isolated VHF pulses are not weak and sometimes comparable in amplitude to the overall VHF emission during the whole flash. Importantly, they are clearly distinguishable in time scale from FPB. These short and isolated VHF pulses may be the same as the so-called "first pulse" reported by Markson and Ruhnke (1999), which were short and temporally isolated from the following pulses, as well as the so called initiating events reported by Marshall et al. (2014), in the form of limited bandwidth, VHF emissions of undetermined duration. Short VHF pulses measured with lower bandwidth instrumentation were also observed at the beginning of four flashes reported by Marshall et al. (2018) and may be the same as the broadband short VHF pulses we describe here. All these consistent and supportive studies suggest that these short and isolated VHF pulses are also a typical class of lightning initiation. Our measurements strongly indicate that FPB is responsible for some lightning initiation, but not all. Assuming that streamers are the source of VHF emissions in both cases, these observations indicate that either a short 10–20 μs burst of streamers in the form of FPB, or a 10–100 times longer duration sequence of isolated streamers is needed in order to generate a fully developed, upward propagating negative leader.

2. VHF Broadband Interferometer System

During the thunderstorm season of 2017, a VHF broadband interferometer system consisting of three sensors was built and deployed at the Duke Forest near Duke University in Durham, NC. Three sensors form two perpendicular baselines of 52-m length, as illustrated in Figure 1a. Each sensor consists of a pair of 16-inch diameter aluminum plates, with the lower plate grounded, and connected to a 13-dB broadband preamplifier and a 55-MHz anti-aliasing low-pass filter. Each sensor forms a vertical electric dipole providing a signal proportional to the time derivative of the vertical electric field across a bandwidth of ~100 kHz to 55 MHz. Small time corrections of 1–2 ns between the three broadband signal channels were measured by using a spark generator at a nearby location whose distance to the three sensors was measured with a laser rangefinder to 1-cm precision. Figure 1a illustrates the basic setup of the sensors at Duke Forest, including the three broadband sensors (CH-1, CH-2, and CH-3) of the interferometer.

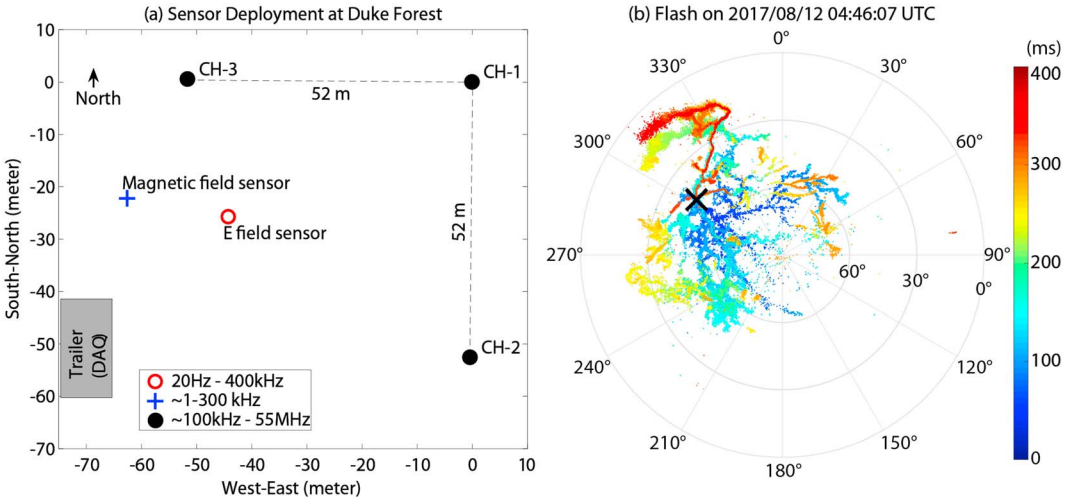

Figure 1. (a) The deployment of the electric field, LF magnetic field, and three broadband interferometer sensors at Duke Forest. (b) An intracloud flash that occurred on 12 August 2017 at 04:46:07 UTC at 4.8-km range and mapped by the broadband interferometer. The color of the dots from blue to red indicate the time of the flash from beginning to the end, while the black cross at azimuth ~300° and elevation ~45° marks the initiation position of the flash. The geographic azimuth (0–360°) is marked by the numbers outside of the circle, while the three circles from outside to inside mark the elevation angle of 0°, 30°, and 60°, with the center being the zenith at the interferometer site.

The simultaneous broadband signals from these three sensors and one GPS IRIG signal were digitized by a 14-bit four-channel data acquisition card (AlazarTech ATS9440) at a sampling rate of 125 megasamples/second (MS/s). The data acquisition initiates on an amplitude threshold trigger, with a pretrigger of at least 200 ms to record the preceding weaker processes before the trigger time. This data acquisition card has an on-board memory of 2 GB and is capable of saving 2-s data for each of the four channels for each trigger, which is long enough to fully capture most lightning flashes. The GPS time is decoded from the simultaneously recorded IRIG time signal. Additional data were provided by a low-frequency (LF) magnetic field sensor (with a proportional (dB/dt) frequency response from ~1 to ~100 kHz and flat frequency response (B) from ~100 to ~300 kHz; Lu et al., 2013) and an electric field change meter (~20 Hz to 400 kHz, time constant of 10 ms) deployed close to the interferometer, as illustrated in Figure 1a. Both were digitized at a sampling rate of 1 MS/s. Note that there is an absolute time uncertainty of several tens of nanoseconds when comparing the VHF interferometer system with the other data acquisition systems synchronized by a different GPS receiver.

Before interferometrically processing the VHF signals, a digital high-pass filter was applied to the raw data to limit the signal frequency band to 20–55 MHz. Then for an entire flash, a short time duration sliding window signal cross correlation (using the method described by Stock et al., 2014) was applied to obtain the time differences between signals from each two sensors. In our study, generally, a 1.5-μs (192 samples) signal processing window with a sliding step of 0.5 μs (64 samples) was used, and a normalized cross-correlation threshold of 0.4 is employed to ensure that the measured time difference corresponds to a real lightning signal instead of noise. Given the bandwidth (35 MHz), typical signal-to-noise ratio (SNR; 10 dB) and processing window width (1.5 μs) of our measurements, the best possible time resolution is approximately 0.2 ns (Stock et al., 2014), and our processing approach goes slightly below that by design. Subsample time resolution of 0.01 ns is obtained by upsampling by a factor of 4 in the time domain and by polynomial fitting to the cross-correlation peak (Stock et al., 2014). After obtaining the time differences from the two perpendicular baselines (ΔT_{12} and ΔT_{13}), the source arrival azimuth (Az) and elevation (El) is found by the following equations (Stock et al., 2014):

$$Az = \tan^{-1}\frac{\Delta T_{12}/d_{12}}{\Delta T_{13}/d_{13}}; \qquad El = \cos^{-1}\left(\sqrt{\left(\frac{c\,\Delta T_{12}}{d_{12}}\right)^2 + \left(\frac{c\,\Delta T_{13}}{d_{13}}\right)^2}\right).$$

Although our system operates at a bit narrower band comparing to the system by Stock et al. (2014), owing to the longer baseline of 52 m, the lower bound of theoretical angular uncertainty (Stock et al.,

2014) in this study is estimated to be around 0.1° at the source elevation of 45° for signals with SNR of 10 dB. This was checked by computing the standard derivation of the mapped sources position comparing to the mean position of a dart leader (which we presume to be a line-like source) at elevation between 45° and 53°. The standard derivation (elevation and azimuth angular uncertainty) was estimated to be 0.17° and 0.26°, respectively, which is consistent with the lower bound theoretical angular uncertainty in this study.

As an example of the performance of the system, Figure 1b shows one IC flash mapped by the VHF interferometer, with the initial breakdown events located by National Lightning Detection Network (NLDN) at 4.8-km horizontal range from the system. The horizontal distance of this flash from the interferometer was estimated from the location of an initial breakdown event reported by NLDN. This is a flash that started with a well-mapped burst of FPB (Rison et al., 2016) and is analyzed in the following section. A total of more than 57,000 VHF sources were identified for this 410-ms duration flash, which is fairly typical for broadband continuous VHF interferometer measurements (Shao et al., 2018; Stock et al., 2014). Both the well-mapped FPB at the initiation of this flash (as illustrated in the follow section) and the clear leader branches demonstrate the good performance of the VHF interferometer used in this study.

3. Measurements and Results

During the thunderstorm season of 2017, there were three storms that produced NLDN-reported IC flashes within 10 km of our system, on 8 July, 12 August, and 24 October. Among all the NLDN-reported flashes recorded during these three close storms, 26 flashes occurred with initial lightning events within 10 km horizontally from the interferometer site. Note that the precise lightning initiation event does not have to be located by NLDN for us to accurately determine its distance, as any NLDN-located lightning event within the first several millisecond of the flash provides a reasonably accurate location of the horizontal position of the flash initiation.

Additionally, in examining the VHF data during these three storms, there also were five other flashes that clearly initiated with very high amplitude, burst-like VHF emissions and simultaneous strong narrow bipolar LF signals time scales of 10–20 μs. These data suggest that they were conventional NBEs, and due to the high amplitude the VHF data are also high quality despite the slightly longer horizontal range (15–20 km) and lower source elevation (~20°). These additional five events are included here for a more comprehensive study of FPB and the VHF emission of lightning initiation events. The resulting data set is a total of 31 IC lightning initiation events, including 26 events within 10 km and another 5 known NBE-FPB events at 15–20 km from the interferometer.

For every flash in this study, the flash initiation event was identified to be the first detectable VHF emission with amplitude at least twice the background noise level, defined as the standard deviation of the VHF emissions during the period without any lightning signals. Based on the initiating VHF, we find that the 31 IC flashes in this data set naturally divide into two populations based on the time scale of the VHF emissions. The initial VHF emissions in one group were a 10–20 μs continuous VHF burst that is essentially identical with the recently identified FPBs (Rison et al., 2016), as we show below. This group includes the 5 NBE-associated events and 3 of the 26 flashes within 10 km of the sensor. Not surprisingly, four of the five NBEs also exhibitied clear fast downward motion of the VHF emissions and dynamics identical to the recently reported FPBs (Rison et al., 2016), with the other one not well resolved.

But the initial VHF emissions in the second group, which includes 23 of the 26 flashes (88%) that initiated within 10 km of our interferometer, contain only very short duration VHF pulses with a typical time scale of 0.5 μs or shorter. These lightning initiation events do not contain any apparent FPB signature. Although it is possible that there is a very weak FPB signature below the noise floor, these events are still fundamentally different from the FPB-initiated flashes in that there are several to several tens of very short VHF pulses that begin tens to hundreds of microseconds prior to the leader initiation. No such short pulses are seen in the eight FPB-initiated IC flashes analyzed here. This indicates that in some cases fast positive breakdown is the process that initiates a lightning flash, but in many and perhaps most cases it is not. In the sections below we show detailed examples of both groups.

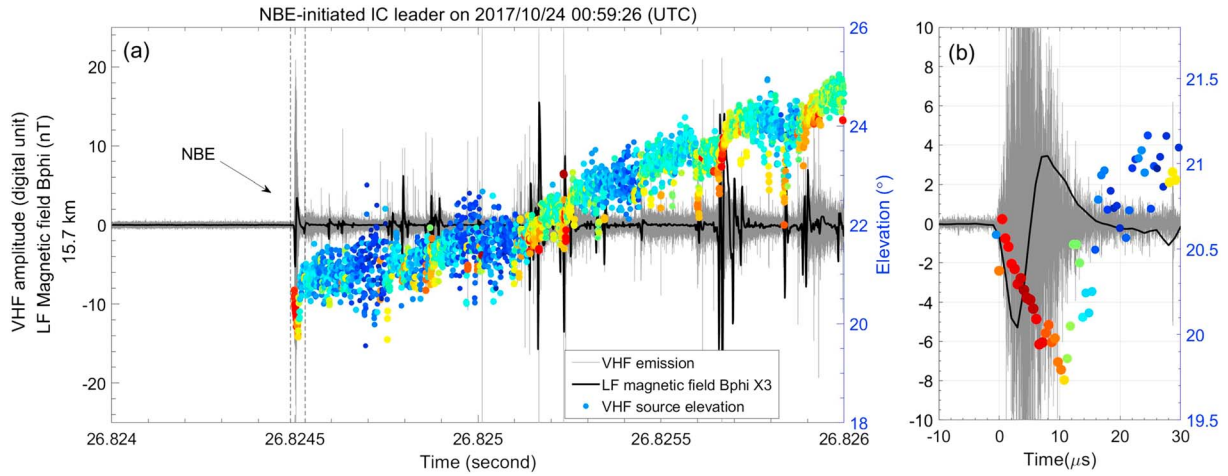

Figure 2. The very high frequency (VHF) emission, low-frequency (LF) magnetic field signal and the interferometer mapped source elevation of intracloud (IC) flashes initiated by an NBE pulse. (a) The overall view development of the IC leader, including the VHF radio emission, LF radio emission, and the VHF source elevation from interferometer in the first 1.5 ms of the IC leader. (b) A zoom-in plot of the time window marked by the dashed lines in (a). The color from blue to red indicates the VHF emission amplitude from weak to strong, with the red color scaled to the strongest source in the showing window. Note that the colors of the VHF sources in the zoom-in figure are rescaled.

3.1. IC Leaders Initiated by Typical Narrow Bipolar Events

As mentioned above, our database contains five typical NBEs (Smith et al., 1999) measured at a range of 15–20 km from the interferometer, four of which exhibit dynamics that are well resolved by the VHF interferometer. Figure 2 shows one example. Similar to what was reported by Rison et al. (2016), this NBE process is composed of strong continuous VHF emission and a bipolar-like LF pulse, both with time scales of approximately 15 μs (note that in the far field, the NBE process may produce a tripolar pulse with a dB/dt sensor). The motion of the VHF emission centroid was clearly resolved, showing fast downward motion followed by ascending development that continuously transitions to an upward negative leader. This NBE was located by NLDN at 15.7 km from the interferometer, and thus we estimate from the elevation angle change a spatial length of the FPB of 280 m, and a propagation speed of the downward positive breakdown estimated to be 2.8×10^7 m/s.

Another three well-resolved NBEs, which were located by NLDN at horizontal distances of 16.8, 18.7, and 19.7 km from the interferometer, share the same basic features as the one shown in Figure 2. The spatial lengths and the propagation speeds of the fast downward positive breakdown were estimated to be 265, 524, and 584 m; and 5.3×10^7, 4.0×10^7, and 4.3×10^7 m/s, respectively. All four well-mapped NBEs were associated with strong continuous burst VHF emission bursts of approximately 15-μs duration and fast downward motion that was followed by upward leader development. All five NBEs in this study (including the one that did not exhibit clear VHF source motion) showed a consistent picture on the time scale and amplitude of the VHF and LF emissions, and overall, these observations and measurements confirm the details of fast positive breakdown, including its association with lightning flash initiation, reported by Rison et al. (2016).

3.2. Three Flash Initiation Events With Weaker Continuous VHF Emissions

Of the 26 flashes that initiated within 10 km of the interferometer and not selected for any feature other than range, only three flashes were initiated with a continuous burst of VHF emissions. The details of these three events are shown in Figure 3. The initial breakdown pulses of these three flashes were located by NLDN at 4.8-, 5.1-, and 6.2-km range from the interferometer and we assume this horizontal range. All three began with continuous VHF emissions of 10- to 20-μs duration, although the VHF amplitude varied significantly, and there is no evidence of any submicrosecond duration short VHF pulses prior to the continuous emissions. Events 1 and 2 were clearly resolved by the interferometer and show downward source motion followed by ascending development. For event 1, it is interesting to note that the downward source motion appears to stop briefly 2 μs after the initiation and then begin again. We conjecture that these dynamics

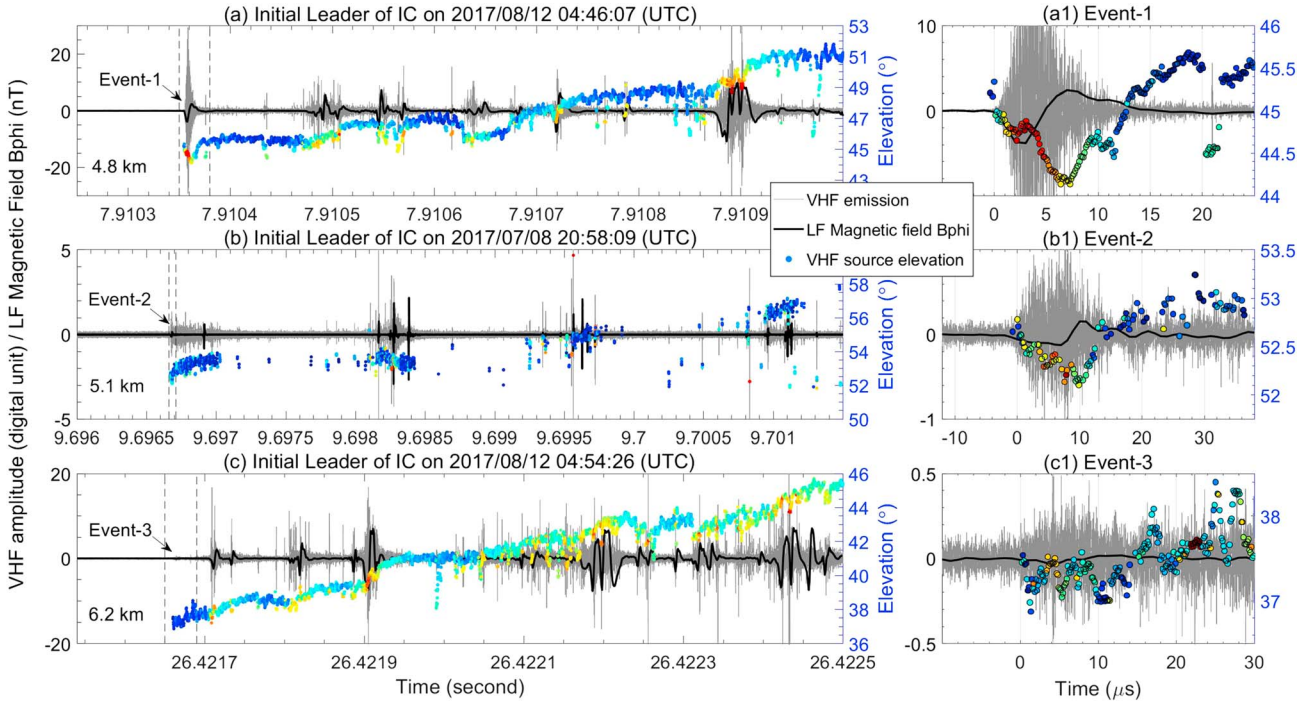

Figure 3. Radio emissions and very high frequency (VHF) interferometer mapping of three intracloud (IC) initial leaders that begin with weak fast positive breakdown. All the signs and scales of the color have the same meaning with that in Figure 2. (a) The initial IC leader on 12 August 2017 at 04:46:07 UTC. (a1) A zoom-in plot of the time window marked by the dashed lines in (a). The signs and plots in (b) and (b1) have the same meaning as (a) and (a1) for the initial leader of IC flash on 8 July 2017 at 20:58:09 UTC. Panels (c) and (c1) show the initial IC leader of a flash on 12 August 2017 at 04:54:26 UTC. Note that the colors of the VHF sources in the zoom-in figure are rescaled.

may reflect inhomogeneity in the background electric field that leads to a slowing and reinitiation of the wave of downward fast positive breakdown.

From the locations of events 1 and 2 estimated with NLDN data, the vertical lengths of the FPB regions were estimated to be 191 and 146 m, respectively, with an overall downward propagation speed of 3.5×10^7 and 1.4×10^7 m/s. All these features, including both the time scale, space scale, downward propagation, and fast speed of the VHF emissions agree well with both the NBE-type and weaker type of FPBs reported by Rison et al. (2016), as well as the NBEs in this study shown in the previous section. Note that, the clear LF pulse of event 1 and the weak pulse-like LF emission of event 2 provide additional evidence that these are strong (event 1) and weak (event 2) FPB events.

Figure 3c shows a third initiation event that contained weak but distinguishable VHF emissions of approximately 10 μs duration, and a very weak LF signal. The VHF interferometer mapping does not resolve well any spatial development of the VHF source because of the relative weak VHF emission. However, the VHF sources in Figure 3c1 still show some downward movement in the first 10 μs followed by the ascending development, as in the other two events shown. We consider this event to also be FPB, although near the lower limit of detectability given the sensitivity of our system.

These were the only 3 out of 26 flashes initiated within 10 km of the interferometer that were started with continuous and downward moving VHF emissions and immediately followed by upward leader development. Both the VHF and LF emissions of these three events spanned a factor of roughly 20 in amplitude, further demonstrating the wide range of the radiation strength of the FPB process (Rison et al., 2016). Collectively, the data for these three events and the five separate NBEs reported here are in excellent agreement with the first description of fast positive breakdown reported by Rison et al. (2016), and together these events solidify a clear and consistent picture of the observable features of FPBs. The key feature is continuous burst of noise-like VHF radiation of 10–20 μs duration that is often resolvable with an emission centroid that moves downward at a speed $>10^7$ m/s. Although FPBs occur with a wide range of VHF amplitudes, and resolving its time development is important for being able to definitively identify FPBs, it may be that a

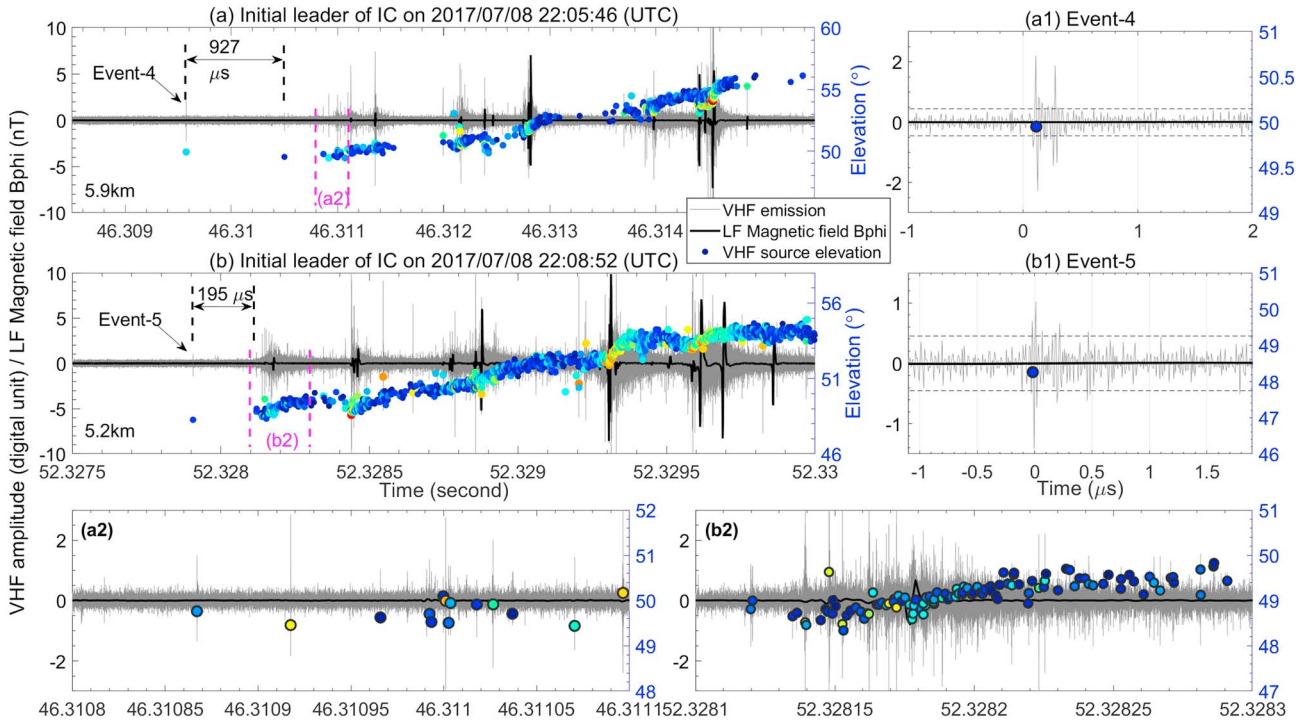

Figure 4. The very high frequency (VHF) emission, low-frequency (LF) magnetic field signal and the interferometer mapped source elevation of two example intracloud (IC) flashes that do not appear to initiate with fast positive breakdown events. Panels (a) and (b) show the first several milliseconds of the initial leaders. Panels (a1) and (b1) show the radio emission and the source location within 1 μs before and 2 μs after the first VHF pulse above the noise threshold. The horizontal dashed lines marked the background noise level. Panels (a2) and (b2) show the radio emissions and source location during the 300 and 200 μs windows marked by the magenta dashed lines in (a) and (b), which bound the VHF emissions at the beginning of continuous upward leader motion. Note that there is a short pulse just after 927 μs of the initiation pulse which share basically the same feature with those VHF pulses in (a2), but it was not included in (a2). All the signs and scales of the color have the same meaning with that in Figure 2. Note that the colors of the VHF sources in the zoom-in figure are rescaled.

10–20 μs continuous burst as the first detectable VHF emission from a lightning flash is sufficient as an identifying signature of fast positive breakdown.

3.3. Flash Initiation Events With Short Pulse-Like VHF Emissions

The remaining 23 flashes that initiated within 10 km of the interferometer (from 1.7 to 10 km) began with VHF emissions that are quantitatively different from the continuous burst of VHF emissions shown in Figures 2 and 3. Figure 4 shows two examples of these initial upward leaders with initial breakdown events located by NLDN at 5.9 and 5.2 km from the interferometer. For both, the first VHF signal above the background noise (marked by events 4 and 5) were very short VHF pulses, with a time scale of less than 0.5 μs, as shown in the Figure 4a1 and 4b1. In addition, at this ~5-km range, no LF emissions were detected above the background noise level by the high gain LF sensor that was originally designed to measure distant (hundreds to thousands of kilometers) lightning signals (Lu et al., 2013). This sequence of events is clearly different from the fast positive breakdown events shown in sections 3.1 and 3.2, even though the peak amplitude of their VHF emissions are comparable.

It is important to emphasize that, as illustrated in Figure 4, these isolated VHF pulses were located by the interferometer at the same points where the continuous upward leaders eventually begin several hundred microseconds later. These short VHF pulses are thus almost certainly connected to the lightning flashes in question. Their very short duration makes them clearly distinct from fast positive breakdown, and, importantly, there are no visible FPB VHF signatures that occur between these initial pulses and the eventual development of an upward leader. For the 23 IC upward leaders initiated by short VHF pulses, the short pulse duration varies from 0.12 to 1.44 μs, with mean/median values of 0.57/0.34 μs. The delay between these VHF pulses and the subsequent continuous leader development ranged from 140 μs to 1.55 ms, with mean/median values of 556/499 μs. One IC flash reported by Marshall et al. (2018) with measurements of electric field change and narrowband VHF also showed a clear gap during the initial *E* field change (IEC

in short) between the first short VHF pulse and the following initial breakdown pulse. For one case in this study, the time gap between the initiation pulse and the following leader was not easy to identify clearly.

It is common for there to be at least several short VHF pulses that occur after the first one and before the initiation of continuous upward leader motion. In a few cases there are as many as several tens of these short pulses spread across the several hundred microsecond time window before the upward leader emerges. As can be seen from the VHF radio emissions in Figure 4, there is some variability in how the short pulses transition into an upward leader. Sometimes it appears through an increasing rate of nonoverlapping short VHF pulses as in Figure 4a2, and sometimes it appears to be an abrupt transition to quasi-continuous VHF emissions as in Figure 4b2. However, we again emphasize that there remains no sign of any 10–20 μs continuous burst of VHF emissions, which would be a signature of FPB, at any point after the initial short VHF pulse.

4. Two Distinct Types of Lightning Initiation Events

The eight events containing fast positive breakdown analyzed in this study show a consistent picture of the spatial and temporal development of the LF and VHF emissions produced in association with FPBs, regardless of the relatively wide amplitude range of the process. As such, this portion of our measurement database is in essentially perfect agreement with the FPB measurements reported by Rison et al. (2016).

However, as illustrated in Figure 4, the first detectable signals from the lightning initiation region for the majority of the lightning initiation events in our database are short (typically <0.5 μs) and isolated VHF pulses. And, in all of these cases, there is no signal that matches the spatiotemporal signature of FPB between the flash initiation and the beginning of the continuous upward leader development. This indicates that fast positive breakdown, as presently understood, does not occur during the initiation of many lightning flashes. Of the 26 flashes selected only by distance that we analyzed, fully, 23 of these (88%) did not have any evidence of fast positive breakdown.

These two classes of lightning initiation are distinguishable in several ways. The first difference, as repeatedly noted above, is the difference of the time scale of the initial VHF emissions. FPB-type VHF emissions have a clear time scale of approximately 10–20 μs duration, as shown in Figures 2 and 3 and by Rison et al. (2016). In other cases, only short and isolated VHF pulses of typically 0.5 μs duration (mean/median value of 0.57/0.34 μs) occur at flash onset, and no FPB-like signal is detectable in the time window between these short pulses and the onset of continuous upward leader development. Also note that all four initiation events in Marshall et al. (2018) measured by LogRF sensor had durations less than 2 μs. This is somewhat slower than the VHF pulses in this study.

The second difference is the occurrence context of the VHF emissions. In the cases with the ultrashort VHF pulses, there is essentially always a significant time delay window in which VHF emissions are either absent or more isolated short pulses until the continuous upward leader development begins. This time delay window is typically several hundred microseconds (mean/median value of 556/499 μs). In contrast, for the eight cases of FPB-initiated lightning shown here, the FPB-type VHF emissions merge continuously into emissions from an upward propagating leader in a time window of several tens of microseconds, with no time window of weak or no VHF activity. The third difference is the lack of detectable LF emission associated with these ultrashort VHF pulse initiation events, even though the VHF emission amplitudes associated with them and some NBE-type events are comparable. This is not surprising given their extremely short duration. Collectively, these three differences suggest that the pulse-like initiation events and the FPBs may represent two distinct types of lightning flash initiation.

If we organize the characteristics of the lightning initiation VHF emissions based on time scale and range-normalized amplitude, the difference is perhaps even clearer. Figure 5 shows the normalized peak amplitude of the VHF emission and the time duration of the initiation events (the time duration of the VHF emission above the background noise level) for all of the 31 initiation events. As marked by the dashed line ellipses in Figure 5, the initiation events in this study can be generally separated into three groups, but with two main types.

Groups A1 and A2 together contain the events with clear fast positive breakdown across a wide range of amplitude. Six of these eight events (excluding the weakest one and one NBE that that had poorly resolved spatial development) share the same spatial and temporal development features, namely 10- to 20-μs

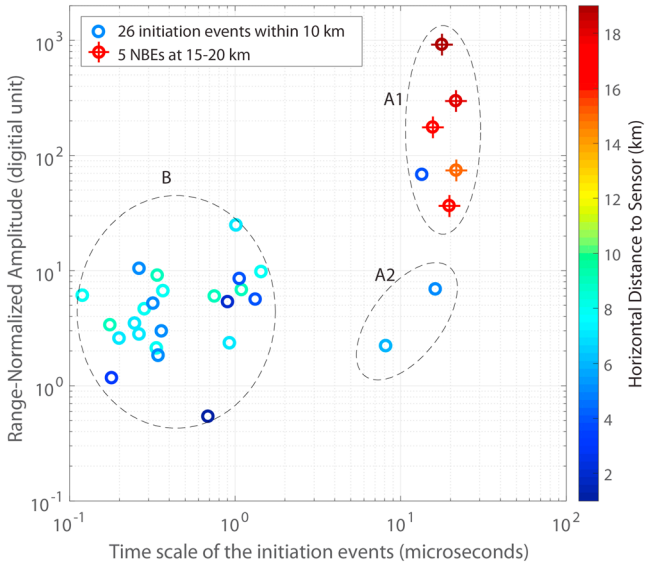

Figure 5. The range-normalized amplitude and time duration of the initial VHF emissions color coded with horizontal range to the sensors. The plot includes the 26 IC flash initiation events that occurred within 10 km of the interferometer, and an additional five NBEs that occurred 15–20 km from the interferometer. Three ellipses indicate the apparent separable groups of initial events. Group A1 includes the six clear and strong fast positive breakdown events, with the five NBEs from 15–20 km and one event at 4.8 km. Group A2 denotes two fast positive breakdown events that had resolvable downward-upward motion and the expected ~10-μs duration VHF emissions, but with a range-normalized amplitude 10 to 100 times smaller than for the NBE events. Group B denotes the second type of event in which the lightning initates with an ultrashort VHF pulse. These short pulses are comparable in amplitude to the VHF emissions from the weaker fast positive breakdown. Importantly, there are no cases with VHF emissions of intermediate time scales. NBE = narrow bipolar event.

duration and clear down-then-up source VHF emission centroid motion. The main difference among these is the amplitude of the VHF emissions. The five known NBEs (section 3.1) and event 1 (section 3.2) produced both strong VHF and LF emissions and are grouped as "strong" FPBs in Group A1. Events 2 and 3 comprise Group A2, which produced VHF and LF emissions but 10 to 100 times weaker than the typical NBEs. However, both the strong and weak versions contain clear 10- to 20-μs bursts of noisy VHF emissions, as noted by Rison et al. (2016).

The VHF emissions during other 23 initiation events in Group B, all within 10 km from the interferometer, are significantly different. They have much shorter VHF duration emission with a typical time scale of less than 0.5 μs, with mean/median values of 0.57/0.34 μs. As shown in Figure 5, the range-normalized amplitude of these short VHF pulses was not as strong as those typical strong version FPBs but is comparable to the weaker FPB events. The difference in time scale alone appears to be enough to separate these two classes of events, and it is remarkable that there are few events for which the VHF emission time scale falls between roughly 1 and 10 μs.

5. VHF Initiation Events, Electric Field Changes and Implications

Figure 6 illustrates examples of these two types of VHF initiation events with the development of LF emissions and the associated electric field (*E* field) change. An FPB-initiating leader occurred at 5.1 km was shown in Figure 6a. The peak VHF emission of this FPB was about one order smaller than that of the typical NBE-type FPB. A bipolar-like LF pulse having basically the same time scale with FPB was observed simultaneously with the FPB. A rapid *E* field change was observed following this FPB with a duration of 0.23 ms before the next clear breakdown pulse, which we interpret as an initial part of the fully formed upward propagating negative leader. Continuous VHF emissions were measured following the FPB event and during the subsequent leader-associated *E* field change, suggesting the existence of continuous active streamer processes during this period, and thus also the possible development of initial leaders. Note that for one NBE-associated FPB example reported by Rison et al. (2016), they indicated that the negative leader had not yet formed in that case, even though the VHF activity following the FPB has extended above the initiation position by several degrees of elevation. We suggest that the occurrence of an FPB initiation event is thus sufficient to create a propagating negative leader in 10–20 μs.

An example of the connection of short and isolated VHF pulse initiation events with a slow *E* field change is shown in Figure 6b. A clear short duration (0.2 μs) VHF event was the first detectable signature of the flash. No detectable LF emissions can be identified, however, a weak and slow *E* field change started after the short VHF initiation event. This electric field change is approximately 100 times slower than the leader-associated field change in Figure 6a, and lasts for 1.55 ms before an initial breakdown pulse and establishment of the propagating leader. We indicate this slow *E* field change is the same process named as initial *E* change (or IEC in short) reported by Marshall et al. (2018). Note that a few additional short duration VHF pulses are detected during the slow *E* field change period and preceding to the following continuous-like leader development, and there may well be additional VHF pulses below the noise threshold. This suggests the possible existence of intermittent streamer initiation that leads to a slow *E* field change, in contrast to the apparent explosive streamer initiation in FPB.

Marshall et al. (2014) and Chapman et al. (2017) investigated the electric field change measurements during the initial breakdown stage of both IC and CG flashes, and reported a slow *E* field change (which they named as initial *E* change, IEC) associated with the initiation of normal flashes. These findings were recently expanded by Marshall et al. (2018) with measurements of electric field change and narrowband VHF

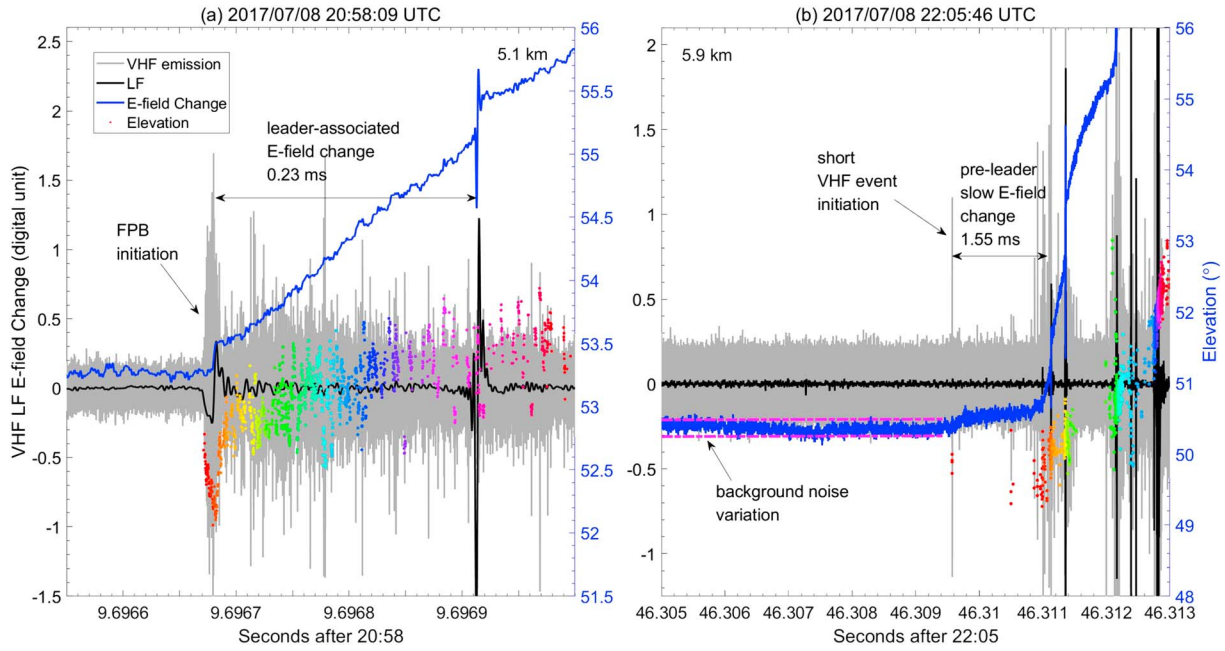

Figure 6. Two examples of electric field change associated with the very high frequency (VHF) initiation events. The VHF emission (gray), low-frequency (LF) magnetic field emission (black), electric field change waveform (blue), and the VHF source elevation (colored dots starting with red) of the initial breakdown process from two flashes occurred at close range are illustrated. Panel (a) show an IC initial leaders started with a relatively weaker fast positive breakdown (FPB) event. Panel (b) shows IC initial leader started with the newly identified short duration VHF event. The two magenta dashed lines in panel (b) marked the background noise variation of the slow *E* field change.

(bandwidth of 186–192 MHz). Marshall et al. (2018) analyzed two intracloud and two cloud-to-ground lightning flashes and found that the IEC initiation was coincident with a short pulse in the LogRF data. Our measurements, with broader bandwidth VHF, more instruments, and many more events, confirm and broaden these findings. We suggest that the IECs reported by Marshall et al. (2014) and Chapman et al. (2017) are the same slow electric field changes that we observe following the short and isolated VHF pulses that initiate the majority of the observed lightning flashes.

6. Conclusions

In this study, we report lightning measurements from a new imaging VHF radio interferometer. After confirming the good imaging performance of the interferometer on complete lightning flashes, we analyzed in detail the VHF radio emissions from the initiation of 31 IC flashes. Of these flashes, 26 were selected for initiation within 10 km of the sensor, and five were selected as known NBEs that initiated from 15- to 20-km range. Two different types of VHF initiation events were distinguished.

One type exhibited clear FPB, in the form of a continuous burst of VHF emissions with time scale of 8–22 μs. The flashes started with downward motion of the VHF emission centroid with a propagation speed of 1.4–6 × 10^7 m/s and merged continuously over several tens of microseconds into upward negative leader development. The features of FPB observed in this study are the same as those reported by Rison et al. (2016), namely a 10- to 20-μs time scale, fast propagation speed, several hundred meters of spatial extent, and a wide range of VHF and LF emission amplitude.

However, the other total of 23 IC lightning initiation events (88% of the 26 selected only through distance from the interferometer) exhibited only several to several tens of short VHF pulses with time scale of typically less than 0.5 μs (mean/median value of 0.57/0.34 μs), which usually began several hundred microseconds before the upward leader fully develops. Results from Marshall et al. (2018) based on less comprehensive measurements of lightning initiation from two IC flashes and two CG flashes are totally consistent with the findings in this study. No spatial development of these short pulse-like VHF emission can be resolved in this study, but all were located at the position where the following continuous upward leaders started. Furthermore, for these flashes that initiated with short VHF pulses, there is no evidence of any

FPB process before (or after) the upward leader development begins. All considered, our measurements confirm that some lightning flashes initiate through fast positive breakdown (Rison et al., 2016), but others (and the strong majority in our dataset) do not.

The simultaneous electric field measurements during these two distinct lightning initiation scenarios shed further light on the underlying processes. Assuming that streamers are the source of VHF emissions in both cases, these observations indicate that either a short 10- to 20-μs burst of streamers, in the form of fast positive breakdown, or a 10–100 times longer duration sequence of isolated streamers, in association with a slow electric field change, is needed in order to generate a fully developed, upward propagating negative leader.

Acknowledgments
The authors would like to acknowledge support from the National Science Foundation Dynamic and Physical Meteorology program through grant AGS-1565606, the DARPA Nimbus program through grant HR0011-10-1-005. This work complies with the AGU data policy. The data are available at Duke Digital Repository with the DOI: https://doi.org/10.7924/r48c9vs2c.

References

Chapman, R., Marshall, T., Karunarathne, S., & Stolzenburg, M. (2017). Initial electric field changes of lightning flashes in two thunderstorms. *Journal of Geophysical Research: Atmospheres*, *122*, 3718–3732. https://doi.org/10.1002/2016JD025859

Cummer, A. S., Lyu, F., Qin, Z., & Chen, M. (2018a). VHF interferometeric imaging of the initiation and propagation of incloud lightning leaders, National Radio Science Meeting, January 4–7, 2018, Boulder, CO.

Cummer, A. S., Lyu, F., Qin, Z., & Chen, M. (2018b). Interferometric radio imaging of the initiation and propagation of in-cloud lightning leaders, 25th International Lightning Detection Conference & 7th International Lightning Meteorology Conference, March 12–15, 2018, Lauderdale, FL.

Griffiths, R. F., & Phelps, C. T. (1976). A model of lightning initiation arising from positive corona streamer development. *Journal of Geophysical Research*, *31*, 3671–3676.

Kawasaki, Z., Mardiana, R., & Ushio, T. (2000). Broadband and narrowband RF interferometers for lightning observations. *Geophysical Research Letters*, *27*(19), 3189–3192. https://doi.org/10.1029/1999GL011058

Le Vine, D. M. (1980). Sources of the strongest RF radiation from lightning. *Journal of Geophysical Research*, *85*(C7), 4091–4095. https://doi.org/10.1029/JC085iC07p04091

Liu, H., Dong, W., Wu, T., Zheng, D., & Zhang, Y. (2012). Observation of compact intracloud discharges using VHF broadband interferometers. *Journal of Geophysical Research*, *117*, D01203. https://doi.org/10.1029/2011JD016185

Lü, F., Zhu, B., Zhou, H., Rakov, V. A., Xu, W., & Qin, Z. (2013). Observations of compact intracloud lightning discharges in the northernmost region (51N) of China. *Journal of Geophysical Research: Atmospheres*, *118*, 4458–4465. https://doi.org/10.1002/jgrd.50295

Lu, G., Cummer, S. A., Li, J., Zigoneanu, L., Lyons, W. A., Stanley, M. A., et al. (2013). Coordinated observations of sprites and in-cloud lightning flash structure. *Journal of Geophysical Research: Atmospheres*, *118*, 6607–6632. https://doi.org/10.1002/jgrd.50459

Markson, R., & Ruhnke, L. (1999). Lightning first pulses used in the "LASI" (time-of-arrival) and "ATLAS" (single station) total lightning mapping systems, Proc. 11th Intn'l. Conf. Atmos. Elec., Guntersville, 188-191.

Marshall, T., Bandara, S., Karunarathne, N., Karunarathne, S., Kolmasova, I., Siedlecki, R., & Stolzenburg, M. (2018). A study of lightning flash initiation prior to the first initial breakdown pulse. *Atmospheric Research*, *217*, 10–23. https://doi.org/10.1016/j.atmosres.2018.10.013

Marshall, T., Stolzenburg, M., Karunarathna, N., & Karunarathne, S. (2014). Electromagnetic activity before initial breakdown pulses of lightning. *Journal of Geophysical Research: Atmospheres*, *119*, 12,558–12,574. https://doi.org/10.1002/2014JD022155

Phelps, C. T. (1974). Positive streamer system intensification and its possible role in lightning initiation. *Journal of Atmospheric and Terrestrial Physics*, *36*(1), 103–111. https://doi.org/10.1016/0021-9169(74)90070-1

Rison, W., Krehbiel, P. R., Stock, M. G., Edens, H. E., Shao, X. M., Thomas, R. J., et al. (2016). Observations of narrow bipolar events reveal how lightning is initiated in thunderstorms. *Nature Communications*, *7*(1), 10721. https://doi.org/10.1038/ncomms10721

Rison, W., Thomas, R. J., Krehbiel, P. R., Hamlin, T., & Harlin, J. (1999). A GPS based three dimensional lightning mapping system: Initial observations in Central New Mexico. *Geophysical Research Letters*, *26*(23), 3573–3576. https://doi.org/10.1029/1999GL010856

Shao, X.-M., Ho, C., Caffrey, M., Graham, P., Haynes, B., Bowers, G., et al. (2018). Broadband RF interferometric mapping and polarization (BIMAP) observations of lightning discharges: Revealing new physics insights into breakdown processes. *Journal of Geophysical Research: Atmospheres*, *123*, 10,326–10,340. https://doi.org/10.1029/2018JD029096

Shao, X. M., Holden, D. N., & Rhodes, C. T. (1996). Broad band radio interferometry for lightning observations. *Geophysical Research Letters*, *23*(15), 1917–1920. https://doi.org/10.1029/96GL00474

Smith, D. A., Shao, X. M., Holden, D. N., Rhodes, C. T., Brook, M., Krehbiel, P. R., et al. (1999). A distinct class of isolated intracloud lightning discharges and their associated radio emissions. *Journal of Geophysical Research*, *104*(D4), 4189–4212. https://doi.org/10.1029/1998JD200045

Stock, M. G., Akita, M., Krehbiel, P. R., Rison, W., Edens, H. E., Kawasaki, Z., & Stanley, M. A. (2014). Continuous broadband digital interferometry of lightning using a generalized cross-correlation algorithm. *Journal of Geophysical Research: Atmospheres*, *119*, 3134–3165. https://doi.org/10.1002/2013JD020217

Sun, Z., Qie, X., Liu, M., Cao, D., & Wang, D. (2013). Lightning VHF radiation location system based on short-baseline TDOA technique—Validation in rocket-triggered lightning. *Atmospheric Research*, *129-130*, 58–66. https://doi.org/10.1016/j.atmosres.2012.11.010

Willett, J. C., Bailey, J. C., & Krider, E. P. (1989). A class of unusual lightning electric field waveforms with very strong high-frequency radiation. *Journal of Geophysical Research*, *94*(D13), 16,255–16,267. https://doi.org/10.1029/JD094iD13p16255